Enhancement of Ultrahigh-Frequency Vibration of Au/Si_3N_4 Composite Resonator with Picosecond Ultrasound

Katsufumi Uehara, Hirotsugu Ogi*, and Masahiko Hirao

Graduate School of Engineering Science, Osaka University, Machikaneyama 1-3, Toyonaka, Osaka 560-8531, Japan

We found that the second through-thickness vibration mode of a gold/silicon-nitride composite thin film is selectively excited by picosecond ultrasound with high efficiency by controlling their thickness ratio. Its mechanical vibration frequency exceeds 50 GHz, being promising for ultrahigh-sensitive mass detector. We developed a theoretical model based on the strain-energy ratio between gold and silicon-nitride layers, and successfully explained the enhancement of the second vibration mode. The sensor chip was applied to detect immobilized proteins through the change in resonance frequency.

An ultrafast light pulse excites subterahertz-frequency acoustic waves in nanoscale materials through impulsive thermal expansion, and they are detected by another ultrafast light pulse through modification of surface dielectric constant (photoelastic effect). This optical pump-probe technique is called picosecond ultrasonic (PSU) method, which was first established by Thomsen and coworkers.[1] Several researchers evolve this method for studying behaviors of ultrahigh-frequency phonons in nanoscale materials. Their achievements include high-frequency surface-wave imaging,[2] evaluation of ultrahigh-frequency acoustic damping,[3,4] thermal excitation of shear waves,[5] discovery of anomalous elasticity of nanomaterials.[6–8]

Recently, PSU method is intensively studied for ultrahigh-frequency oscillators: A resonator can be a mass-sensitive sensor because its resonance frequencies are changed by the mass-loading effect, and the mass sensitivity becomes significantly higher as the resonator mass decreases, corresponding to higher-frequency resonator. Because the PSU method allows excitation of ultrahigh-frequency vibrations of nanoscale materials, it is promising for ultrahigh-sensitive sensors. Surface acoustic wave resonances were detected by fabricating nanowires[9–11] and nanodots[12] on substrates, achieving ∼10 GHz resonators. Ultrafast vibrations (∼10 GHz) of GaAs nanopillars[13] and Au nanorings[14] were also successfully realized. In these methods, however, there is a frequency limitation caused by the lithography fineness. Furthermore, they require multistep fabrication procedures costly. The simplest resonator is a flat thin film, whose resonant frequencies can be easily increased by thinning the deposited film. The thin-film resonator were actually utilized for biosensors for detecting target proteins.[15] The disadvantage of the deposited thin-film resonator is significant vibrational-energy leakage

into the substrate. We then developed a locally free-standing film resonator.[16] However, to keep the sensor surface flat, the film thickness should exceed 100 nm, limiting its fundamental resonance frequency. Thus, a methodology for selectively exciting higher resonant modes is desired. We here find that the second through-thickness resonant mode, exceeding 50 GHz, were selectively and effectively excited in a gold/silicon-nitride composite thin film by controlling their thickness ratio and discuss the mechanism using the strain-energy distribution. Finally, we demonstrate its ability as an ultrahigh-sensitive biosensor.

We developed free-standing Au/Si_3N_4 thin films deposited on Si substrate. Si_3N_4 is a nearly transparent, and we needed a metallic thin film as the vibrational source in the PSU method. Au is suitable in this purpose, because it shows high affinity to thiol terminals, through which receptor proteins can be immobilized on the Au surface. First, We deposited Si_3N_4 thin film (80-120 nm) on a (001) Si substrate (7×7 mm^2) by the chemical-vapor-deposition method. Second, we removed the center rectangular part of the Si substrate (2×2 mm^2) by the anisotropic etching with a potassium-hydroxide solution to fabricate partially free-standing resonator. Finally, Au film (10-40 nm) was deposited on the Si_3N_4 surface by the magnetron sputtering method.

We developed the optics for the PSU method with a stable fiber laser instead of titanium-sapphire (Ti/S) pulse lasers, which have been previously used in PSU studies. Our system has two advantages: First, the power stability of the fiber laser is much better than a Ti/S pulse laser, being more suitable for sensor applications. Second, the optics system can be compacted. In this system, the linearly polarized light pulse of 1064 nm wavelength with 150 fs duration was frequency-doubled to obtain visible 532 nm light pulse, and it was divided into the pump and probe light pulses using a polarizing beam splitter (PBS). The pump light was focused at the Au/Si_3N_4 interface from the Si_3N_4 side, which excited vibrations of the composite thin film through the impulsive thermal expansion. The time-delayed probe light pulse was also focused on the interface from the Si_3N_4 side. (The light pulses irradiated the Au layer from the back side so as to prevent them from affecting proteins immobilized on the Au surface.) Powers of pump and probe lights were 5 mW. The probe light pulse reflected from the resonator film was filtered by another PBS and detected by a balanced photo detector. The intensity of pump light was modulated at 1 MHz by an acousto-optic modulator. The baseline-subtracted output from the detector entered a lock-in amplifier, which extracted the modulation-frequency components, providing information on vibrations of the resonator. The vibrational waveforms can be obtained through the reflectivity change of the probe light pulse via the photoelastic effect. Details of the optics appear elsewhere.[17]

Figures 1 (a) and (b) show time-resolved reflectivity changes of probe light pulse for two composite thin films with different thickness ratios. In the case of 15.5 nm Au/120 nm Si_3N_4 composite film, the waveform appears to involve various modes, and the signal-to-noise (S/N)

ratio is lower. Its Fourier transform spectrum (Fig. 1(c)) consists of more than three modes. Such a highly interfering signal is inapplicable to sensor applications because the acoustical energy in an intended mode reduces due to multimode excitation. On the other hand, the film composed of 30 nm Au and 100 nm Si_3N_4 yielded a single-frequency vibration as shown in Fig. 1(b), and its S/N ratio is much higher. Its Fourier spectrum indeed shows a single peak at 55 GHz. Thus, the detectable modes highly sensitive to the thickness ratio.

For identifying the observed modes, we calculated the resonance frequencies of the multilayer films with the stress-free conditions at the top and bottom surfaces and the continuity of stress and displacement at the interface.[18] Used parameters were as follows: the mass density and the longitudinal-wave velocity (along [111] direction) for Au were 19280 kg/m^3 and 3445 m/s, and those for Si_3N_4 were 3200 kg/m^3 and 10111 m/s.[19] The calculated resonance frequencies are shown with vertical broken lines in Figs. 1 (c) and (d), showing a good agreement with measurement: It is revealed that the single vibrational mode in Fig. 1(d) is the second through-thickness resonance.

We explain the dependence of detectable vibrational mode on the thickness ratio with the strain energy distribution throughout the composite resonator. Figures 2(a) and (b) show the distributions of the maximum strain energy per unit volume at individual points up to the third modes in the two resonators in Figs. 1(a) and (b), respectively. The energy absorption depth of the pump light of 532 nm for Au is evaluated to be 17.6 nm from the extinction coefficient. When it irradiates the Au film through the Si_3N_4 film, the strain energy caused by the thermal stress accumulates in the absorption region of Au film. We note that the second mode of the 30 nm Au/100 nm Si_3N_4 resonator causes a large strain energy in this absorption region, while the strain energy in the Si_3N_4 region is lower (Fig. 2(b)). Thus, the second mode of this composite film is expected to be efficiently excited. In the case of the the 15.5 nm Au/120 nm Si_3N_4 resonator, however, the strain energy is not localized in the pump-light absorption region, and it broadly distributes throughout the resonator (Fig. 2(a)). This trend is similar to those of other modes, and not only the second mode but also other modes can be excited with nearly equal efficiency. For quantitative evaluation of this phenomenon, we calculate the ratio of integrated values between in the light absorbed region and in the Si_3N_4 film as the strain-energy localization parameter (SELP) as illustrated in Fig. 3. The SELP indicates the degree of strain-energy accumulation at the light absorption region for an intended mode, and it will correlate with the second-mode selectivity. Figure 4 compares the theoretically calculated SELP value and the ratio of second-mode peak height with that of the fundamental mode in the observed Fourier spectra, which represents the experimental second-mode selectivity. Their trends agree with each other, indicating that our explanation applies essentially. However, we note that electrons excited by the pump light pulse will diffuse before fully transferring their energy to the lattice in a material with weak electron-phonon

interaction like gold, and that this phenomenon affects the strain-field distribution created by the thermal stress.[20,21] We will therefore consider this effect for achieving more quantitative agreement in future.

Finally, we demonstrate the usefulness of the mode-selective ultrathin-film oscillator as a protein sensor. We immobilized anti rabbit-immunoglobulin-G antibody on the Au surface using a self-assembled monolayer. The immobilization procedure was identical to that in our previous study.[15] We measured the waveforms and resonance frequencies before and after the protein immobilization in atmosphere. The results are shown in Fig. 5. The resonance frequency decreased by 4.2% with the immobilization of protein. This immobilization caused a frequency decrease of the order of 0.01% with our high-sensitive wireless-electrodeless biosensor with a 170-MHz quartz resonator.[22] Thus, two-orders-of-magnitude amplification in the mass sensitivity is made possible with this ultrahigh-sensitive film oscillator. Although the quality factor of the ultrathin-film resonator is much worse, it will be improved by decreasing defects in the silicon-nitride film with thermal treatments. More importantly, the technique presented here can achieve a large-scale multichannel sensor because the sensing area can be decreased to 1×1 μm^2, giving significant contributions in the high-throughput screening in drug-development processes.

In summary, we successfully developed a methodology to selectively excite and detect a single-mode vibration of a free-standing Au/Si_3N_4 resonator at frequencies higher than 50 GHz. The detectable mode was highly dependent on the thickness ratio between Au and Si_3N_4 films; the most favorable thickness ratio was 0.3. We attributed this phenomenon to the localization of the strain-energy at the light-absorption region in Au for the specific mode and theoretically reproduced this trend. The ability of the developed 55-GHz resonator as a protein sensor was demonstrated by immobilizing proteins on the Au surface, which caused more than 4% frequency decrease.

Acknowledgement

This study was supported by Funding Program for Next Generation World-Leading Researchers (Next Program) by cabinet office, Government of Japan.

References

1) C. Thomsen, H. T. Grahn, H. J. Maris, and J. Tauc: Phys. Rev. B **34** (1986) 4129.

2) Y. Sugawara, O. B. Wright, O. Matsuda, M. Takigahira, Y. Tanaka, S. Tamura, and V. E. Gusev: Phys. Rev. Lett. **88** (2002) 185504.

3) P. Emery and A. Devos: Appl. Phys. Lett. **89** (2006) 191904.

4) C. Ferrante, E. Pontecorvo, G. Cerullo, A. Chiasera, G. Ruocco, W. Schirmacher, and T. Scopigno: Nat. Commun. **4** (2013) 1793.

5) O. Matsuda, O. B. Wright, D. H. Hurley, V. E. Gusev, and K. Shimizu: Phys. Rev. Lett. **93** (2004) 095501.

6) H. Ogi, M. Fujii, N. Nakamura, T. Yasui, and M. Hirao: Phys. Rev. Lett. **98** (2007) 195503.

7) N. Nakamura, H. Ogi, T. Yasui, M. Fujii, and M. Hirao: Phys. Rev. Lett. **99** (2007) 035502.

8) K. Tanigaki, H. Ogi, H. Sumiya, K. Kusakabe, N. Nakamura, M. Hirao, and H. Ledbetter: Nat. Commun. **4** (2013) 2343.

9) G. A. Antonelli, H. J. Maris, S. G. Malhotra, and J. M. E. Harper: J. Appl. Phys. **91** (2002) 3261.

10) A. A. Maznev: Phys. Rev. B **78** (2008) 155323.

11) H. Ogi, A. Yamamoto, K. Kondou, K. Nakano, K. Morita, N. Nakamura, T. Ono, and M. Hirao: Phys. Rev. B **82** (2010) 155436.

12) J.-F. Robillard, A. Devos, I. Roch-Jeune, and P. A. Mante: Phys. Rev. B **78** (2008) 064302.

13) H. Sakuma, M. Tomoda, P. H. Otsuka, O. Matsuda, O. B. Wright, T. Fukui, K. Tomioka, and I. A. Veres: Appl. Phys. Lett. **100** (2012) 131902.

14) T. A. Kelf, Y. Tanaka, O. Matsuda, E. M. Larsson, D. S. Sutherland, and O. B. Wright: Nano Lett. **11** (2011) 3893.

15) H. Ogi, K. Matsumoto, Y. Fujita, T. Kawamoto, N. Nakamura, and M. Hirao: Appl. Phys. Express **3** (2010) 017001.

16) H. Ogi, T. Kawamoto, N. Nakamura, M. Hirao, and M. Nishiyama: Biosen. Bioelectron. **26** (2010) 1273.

17) H. Ogi, T. Kawamoto, Y. Nakamichi, and M. Hirao: Jpn. J. Appl. Phys. **51** (2012) 07GA08.

18) H. Ogi, Y. Fukunishi, T. Omori, K. Hatanaka, M. Hirao, and M. Nishiyama: Anal. Chem. **80** (2008) 5494.

19) K. J. Singh, Y. Matsuda, K. Hattori, H. Nakano, and S. Nagai: Ultrasonics **41** (2003) 9.

20) O. B. Wright: Phys. Rev. B **49** (1994) 9985.

21) G. Tas and H. J. Maris: Phys. Rev. B **49** (1994) 15046.

22) H. Ogi: Proc. Jpn. Acad., Ser. B **89** (2013) 401.

Figure Caption

Fig. 1 Reflectivity changes observed from (a) 15.5 nm Au/120 nm Si_3N_4 resonator and (b) 30 nm Au/100 nm Si_3N_4 resonator, and their corresponding Fourier spectra (c) and (d), respectively. Vertical broken lines are resonance frequencies calculated by the multi-layer model. Schematic of a cross-section view of the partially free-standing film is shown in (a).

Fig. 2 Distributions of the maximum strain energy per unit volume for first three through-thickness-resonance modes for (a) 15.5 nm Au/120 nm Si_3N_4 and (b) 30 nm Au/100 nm Si_3N_4 resonators. The distributions are normalized by their maxima. Vertical broken lines indicate the interface.

Fig. 3 Schematic for calculating the strain-energy localization parameter (SELP) of the second vibrational mode from the strain-energy distribution. .

Fig. 4 Comparison of the calculated strain-energy localization parameters (SELP) and the observed second-mode amplitude (normalized by the fundamental-mode amplitude). Solid lines are guides to indicate their trends.

Fig. 5 (a) Waveforms before and after immobilization of the protein on the Au surface and (b) their Fourier spectra. An enlarged view near the peak is shown in the inset. (c) The resonance frequencies before and after the protein immobilization.

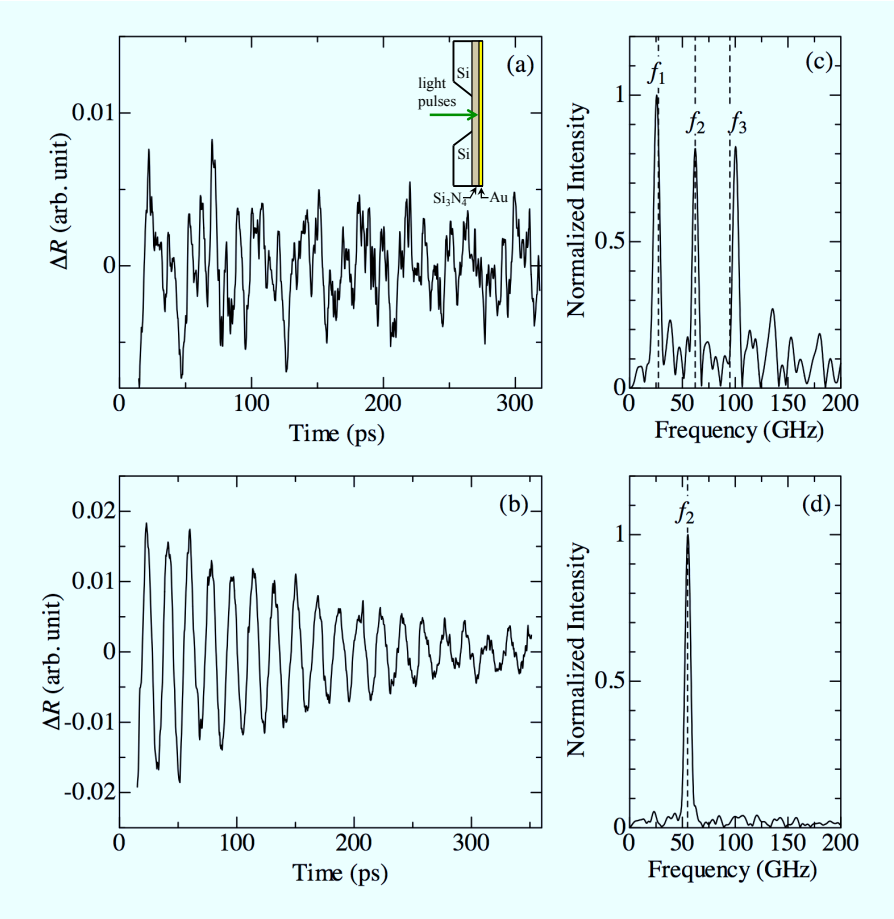
(a)
light pulses
Si
Si
Si_3N_4
Au
ΔR (arb. unit)
Time (ps)
(b)
ΔR (arb. unit)
Time (ps)
(c)
f_1
f_2
f_3
Normalized Intensity
Frequency (GHz)
(d)
f_2
Normalized Intensity
Frequency (GHz)

Fig. 1.

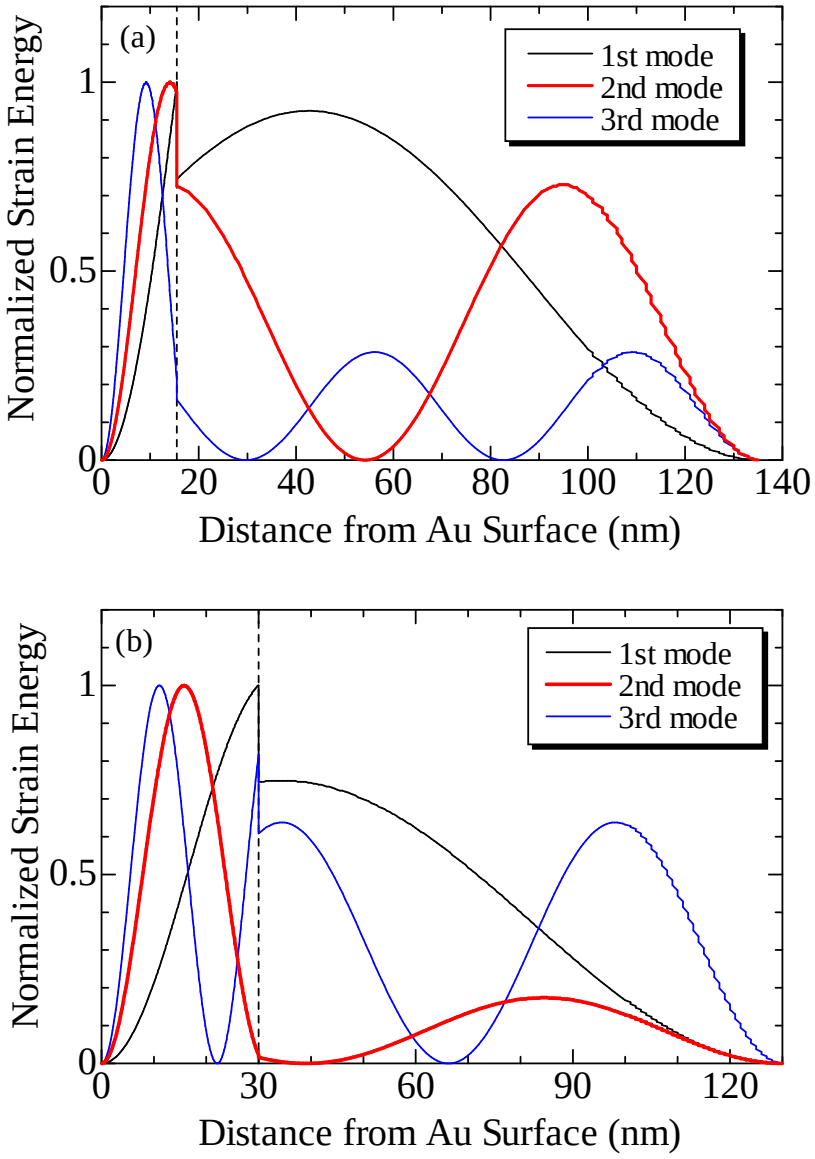
(a)
1st mode
2nd mode
3rd mode
Normalized Strain Energy
0
0.5
1
0
20
40
60
80
100
120
140
Distance from Au Surface (nm)
(b)
1st mode
2nd mode
3rd mode
Normalized Strain Energy
0
0.5
1
0
30
60
90
120
Distance from Au Surface (nm)

Fig. 2.

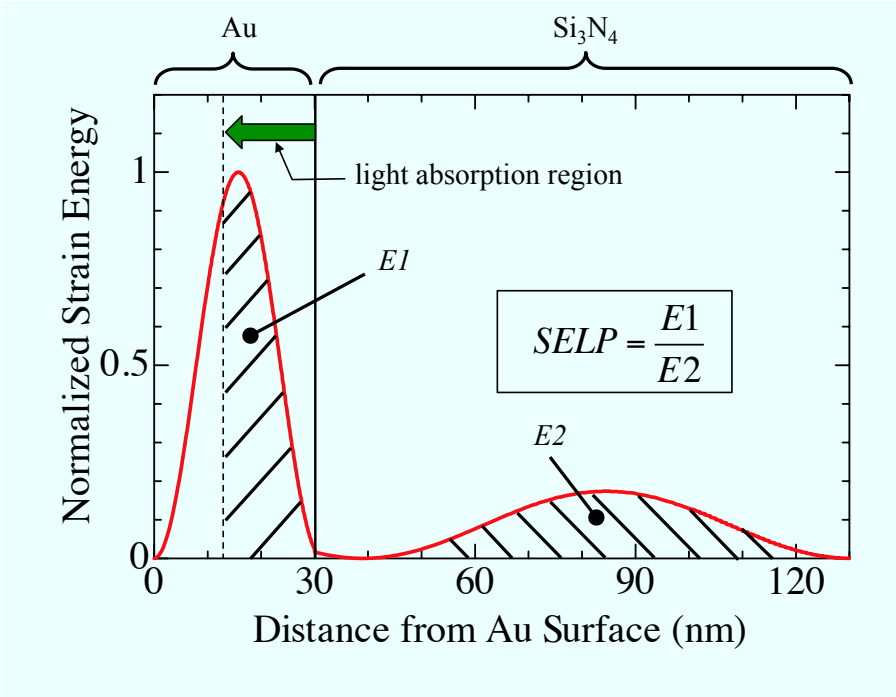
Au
Si3N4
Normalized Strain Energy
1
0.5
0
light absorption region
E1
E2
SELP = E1/E2
0
30
60
90
120
Distance from Au Surface (nm)

Fig. 3.

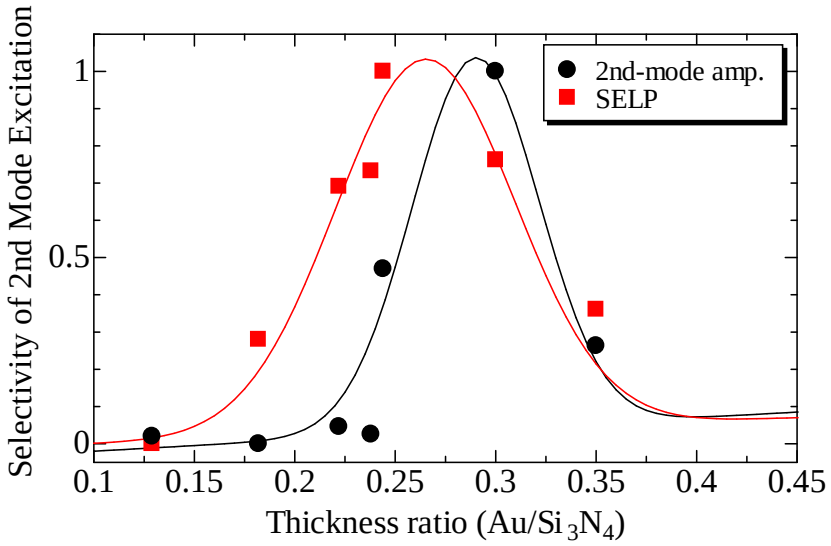
Selectivity of 2nd Mode Excitation
1
0.5
0
0.1
0.15
0.2
0.25
0.3
0.35
0.4
0.45
Thickness ratio (Au/Si 3N4)
2nd-mode amp.
SELP

Fig. 4.

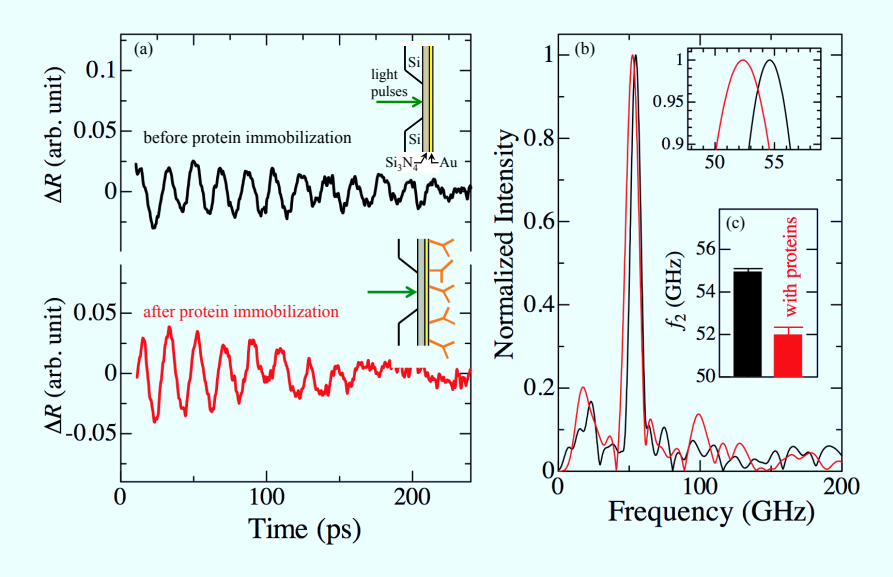
(a)
before protein immobilization
after protein immobilization
light pulses
Si
Si
Si_3N_4
Au
ΔR (arb. unit)
Time (ps)
(b)
Normalized Intensity
Frequency (GHz)
(c)
f_2 (GHz)
with proteins

Fig. 5.